SOUNDING ROCKETS AS A REAL FLIGHT PLATFORM FOR AEROTHERMODYNAMIC CFD VALIDATION OF HYPERSONIC FLIGHT EXPERIMENTS

Andreas Stamminger[(1)], John Turner[(2)], Marcus Hörschgen[(3)], Wolfgang Jung[(4)]

[(1)]Mobile Rocket Base, DLR, Oberpfaffenhofen, 82234 Wessling, Andreas.Stamminger@dlr.de
[(2)]Mobile Rocket Base, DLR, Oberpfaffenhofen, 82234 Wessling, John.Turner@dlr.de
[(3)]Mobile Rocket Base, DLR, Oberpfaffenhofen, 82234 Wessling, Marcus.Hoerschgen@dlr.de
[(4)]Mobile Rocket Base, DLR, Oberpfaffenhofen, 82234 Wessling, Wolfgang.Jung@dlr.de

ABSTRACT

This paper describes the possibilities of sounding rockets to provide a platform for flight experiments in hypersonic conditions as a supplement to wind tunnel tests. Real flight data from measurement durations longer than 30 seconds can be compared with predictions from CFD calculations. This paper will regard projects flown on sounding rockets, but mainly describe the current efforts at Mobile Rocket Base, DLR on the SHarp Edge Flight EXperiment SHEFEX.

1. INTRODUCTION

The Mobile Rocket Base, DLR has experience in launching sounding rockets over four decades. During their suborbital parabolic flight, sounding rockets reach altitudes of up to more than 1000 km depending on requirements. The majority of sounding rockets have been used for experiments which require exoatmospheric trajectories, as for example astronomy and micro-gravity experiments. Micro-gravity conditions are necessary for some technology, material science and biology experiments. In the past, sounding rockets have also been used for measurements in high atmosphere (mesosphere).

For hypersonic reentry experiments on sounding rockets the experiment phase is moved from the exoatmospheric phase to the atmospheric reentry on the down-leg of the trajectory. In this case the vehicle comprises the last stage of the rocket and the hypersonic experiment. On the up-leg the experiment is covered with a nosecone. The goal of such configurations is to establish a low-cost option for a “flying wind tunnel” providing real flight environment.

An example for reentry experiments on sounding rockets is the NASA Sub-Orbital Aerodynamic Reentry EXperiment SOAREX program to test future flight vehicles. SOAREX-1 was launched in 1998 on a Mk70 Terrier / BlackBrant IX rocket with a payload of 11 separate hypersonic experiments. It reached an apogee of 290 km and ejected each experiment at 4 second intervals [NASA, 2004]. SOAREX-2 was launched in 2002 on a newly developed hybrid rocket to achieve Mach 5 during the reentry. The payload included a wave rider flying wedge, a hypersonic parachute and a Slotted Compression Ramp Probe SCRAMP that is a superstable reentry probe [8].

Another example for a sounding rocket flight that adopted this concept is the HyShot experiment of the University of Queensland. The goal was to correlate data of a super combustion experiment in shock tunnel and in flight conditions. After a failure of the first flight in 2001, super combustion was achieved in the second flight in 2002. The two-staged rocket consisted of a Terrier as booster and an Orion motor as 2nd stage. For the reentry the burnt out Orion motor remained attached to the scramjet module to ensure flight stability during reentry.

The HyShot vehicle achieved an apogee of 315 km. Its attitude had to be adjusted to point downwards in flight direction during reentry, to ensure that the aerodynamic loads on the fins are not too high and the vehicle is not decelerated to fast. The HyShot vehicle used cold gas thrusters with nitrogen to perform a bang-bang maneuver where small pulses induce precession on the spinning vehicle. In an altitude from 35 km to 23 km it achieved Mach numbers between 7.6 and 7.8 [2], [9].

SHEFEX is a hypersonic experiment that will be flown on a sounding rocket, similar to the HyShot concept. In this paper the differences of the SHEFEX mission to a conventional sounding rocket mission are explained and the necessary changes in design to provide stable reentry behaviour are pointed out.

2. TYPICAL SOUNDING ROCKET MISSION SEQUENCE

Because most low cost rockets are spin-stabilized during ascent, the payload usually has to be de-spun before the experiment time. The experiment phase starts usually at an altitude of 100 km [5].

To provide better recovery conditions the payload has to reduce the speed during reentry. The payload is spun up again and switches due to aerodynamic disturbances to a flat spin mode. Because of the flat

spin the cylindrical payload creates a higher aerodynamic drag than a cylinder where the air flow is parallel its longitudinal axis. For approximations it is possible to use following c_D coefficients, where the reference area is the cross-sectional area:

c_D = 0.9 for a cylinder with the longitudinal axis parallel to the air flow

c_D = 1.2 for a cylinder with the longitudinal axis perpendicular to the air flow

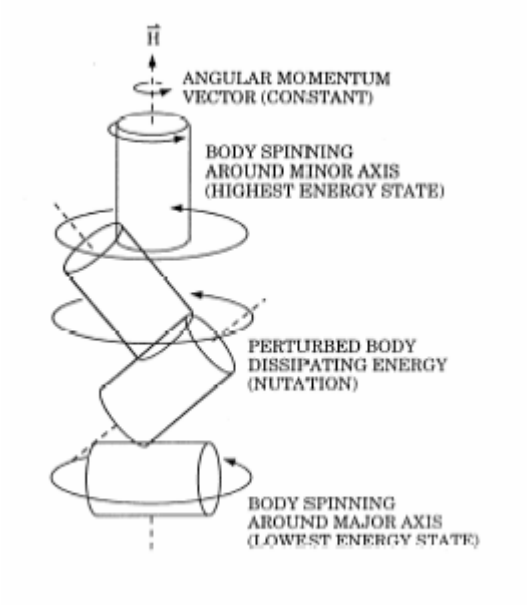

Fig. 1: Introduction of Flat Spin because of Energy Dissipation [1]

Therefore it has to be ensured that the center of gravity of the cylindrical payload is close to the geometric centre of the payload to avoid a stable entry. When it enters the atmosphere, the aerodynamic drag induces small torques on the spinning payload. Regarding the energy, a body that spins about the axis with the smallest moment of inertia has the maximum rotation energy if the angular momentum is constant. Because of energy dissipation, nutation is induced on the payload and the total energy decreases until the payload has reached the minimum rotation energy. This is the case when the cylindrical body spins about the axis with the highest moment of inertia [7].

Due to the flat spin, the descent velocity decreases to 120-160 m/s in approximately 6 km altitude, where the recovery sequence is activated by deployment of the stab chute.

The Mach numbers during reentry depend mainly on the apogee, respectively payload mass. The two-staged rocket of the Brazilian “Baronesa”-mission, with similar motor configuration as the SHEFEX rocket, achieved an apogee of more then 300 km and has reached Mach numbers up to 7.8 between 100 an 30 km on descent [3]. The maximum deceleration of approximately 18 g appears at approximately 30 km altitude for a two-staged vehicle [5].

3. SHEFEX

The SHEFEX project is conducted under the responsibility of the DLR and uses the capabilities and knowledge of the Institute of Aerodynamics and Flow Technology, the Institute of Structures and Design and the Mobile Rocket Base that is responsible for the test flight of SHEFEX.

The aim of SHEFEX is to investigate the behaviour and possibilities of a new shape for reentry vehicles comprising sharp edges and facetted surfaces. Another object is the correlation of numerical analysis and real flight data in terms of aerodynamic effects and structural concept for the thermal protection system. With the SHEFEX mission, the DLR gains the capability to open the opportunity for new low-cost hypersonic experiments on sounding rockets that can be a supplement to wind tunnel test and CFD calculations.

The vehicle consists of a Brazilian S30 motor as first stage and an Improved Orion motor as second stage. This motor configuration has been launched successfully two times and reached with a hammerhead configuration an altitude of 320 km [3]. Basically the same rocket configuration was foreseen for SHEFEX (Fig. 2).

Fig. 2: First Design Approach for the Vehicle from existing Components

The use of mainly available components makes it possible to realize this challenging flight as a low-cost mission. Due to stability problems occurred during the development process, changes in vehicle design have become necessary. The launch of the rocket will be from the Andøya Rocket Range, Norway.

3.1 THE EXPERIMENT

The primary structure of SHEFEX is an aluminum frame and the surface of the experiment consists of flat panels of different materials and surface coatings for thermal protection. Fig. 3 shows the facetted body of the SHEFEX experiment mounted on the payload section of the rocket with an interface module that provides the transition from the asymmetric cross section of SHEFEX to the cylindrical payload modules.

More information on the experiment and the measurements that will be performed during the hypersonic reentry can be found in [4] and [10].

An important design issue of the SHEFEX body is its asymmetric shape. During the reentry this asymmetry induces lift and moment about the pitch axis on the vehicle. Several changes in the design from the first concept were necessary to ensure flight stability.

Fig. 3: Mock-up of SHEFEX

3.2 MISSION SEQUENCE

3.2.1 ASCENT PHASE

The vehicle is accelerated by the S30 motor for 28 seconds until burnout at an altitude of 17 km. At burnout of the first stage the vehicle has already reached a velocity of 930 m/s, respectively Mach 3.17. The fins of the 1st stage are canted and induce a spin rate of approximately 1 Hz for stabilization.

In the coast phase that lasts for 8 seconds the 2nd stage separates from the S30 motor. To keep the complexity low, the layout of the separation system is passive. Until now the launched rockets of this motor configuration were separated due to atmospheric drag only (see Fig. 2). The diameter of the S30 motor (557 mm) is larger than the Improved Orion motor (356 mm) and therefore the 1st stage has enough face surface to ensure a non problematic separation. Because of several changes that had to be performed on the design of the SHEFEX vehicle to ensure a stable reentry flight, a passive system based just on atmospheric drag was assumed not to be sufficient. Studies and layout changes in the design of the separation system were necessary to ensure a smooth separation. These are discussed in chapter 3.3.3.

The ignition of the 2nd stage (Improved Orion) is 36 seconds after launch. After burnout, the 2nd stage will not be separated from the payload but will, after the separation of the nose ogive fairing, comprise the configuration during atmospheric reentry. Calculations were performed to ensure a stable ascent of the vehicle, normally spin stabilized by canted fins on both stages. As a non-spinning flight for the experiment phase is required, the 2nd stage fins may not be deflected, complicating the flight dynamics throughout the up-leg. All modifications on the experiment configuration affect also ascent behaviour.

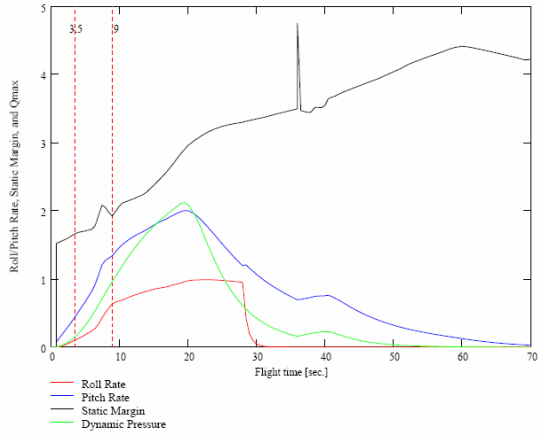

Fig. 4: Roll Rate and Static Margin during Ascent

3.2.2 EXOATMOSPHERIC PHASE

In the current design status, the SHEFEX vehicle will reach an apogee of approximately 280 km.

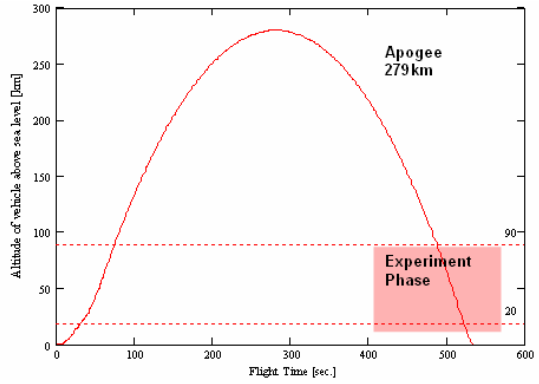

Fig. 5: Flight Trajectory for the SHEFEX Vehicle with a Mass of 350 kg

In the exoatmospheric phase the Attitude Control System (ACS) will align the reentry body, consisting of the experiment and service systems attached to the burnt out Improved Orion motor such that the reentry attitude provides a nominal zero angle of attack for the SHEFEX experiment. During the ascent and after burnout of the 2nd stage, the vehicle will have reduced its spin rate to approximately one half revolution per second. At approximately 100 km altitude when the aerodynamic drag has reduced to a negligible level, the ACS will remove the remaining spin of the vehicle and align the vehicle pitch plane with the trajectory plane. The vehicle will then be rotated in this plane such that the longitudinal axis is aligned with the instantaneous flight direction (See chapter 3.3.4).

3.2.3 REENTRY / EXPERIMENT PHASE

The experiment phase begins at an altitude of 90 km on the down-leg. The stable atmospheric reentry differs from the conventional tumbling motion of the flat-spinning payload that is usual for standard sounding rocket missions. See also chapter 2. The asymmetric shape of the SHEFEX experiment and the resulting lift-force and pitching-moment lead to a non-zero trim angle.

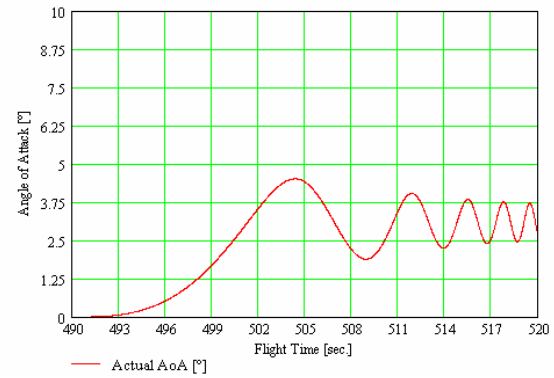

Fig. 6: Pitching Oscillation Movement of the vehicle during Reentry

In order to find an aerodynamic stable configuration for the reentry it was necessary to investigate several variations in vehicle design by means of CFD calculations and semi-empirical tools. This development process and the result that leads to a flare concept for the tailcan of the Improved Orion motor are described in chapter 3.3.1.

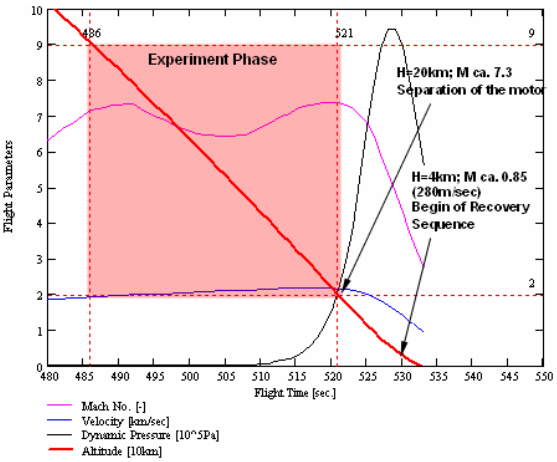

Fig. 7: Reentry Parameter for the SHEFEX Vehicle with a Mass of 350 kg

During the descent and at the start of reentry, the control torques provided by the ACS are capable of correcting the initial aerodynamic disturbing torques in all axes, but the asymmetric experiment form will fairly quickly provide disturbances which greatly exceed the thrust capability of the control system in the lateral axes. As the roll asymmetry is much less the anticipated roll disturbances are considerably smaller and the ACS roll torques also much greater such that the system may be commanded to disable lateral control but continue roll control.

During the experiment phase the vehicle will reach velocities between mach 6 and Mach 7.3 depending on the apogee, respectively vehicle mass.

Because of the higher thermal strains during stable reentry it was necessary to develop a new blade antenna to ensure continuous transmission of sensor and experiment data. This is discussed in chapter 3.3.5.

The experiment phase will end at an altitude of 20 km with the separation of the payload from the 2nd stage motor under hypersonic conditions. The payload module with the SHEFEX experiment will skip to an instable flight and decelerate to a recovery velocity of approximately 230 - 280 m/s. Fig. 8 shows the velocity during reentry, with a change from a stable to instable flight at 20 km altitude after separation.

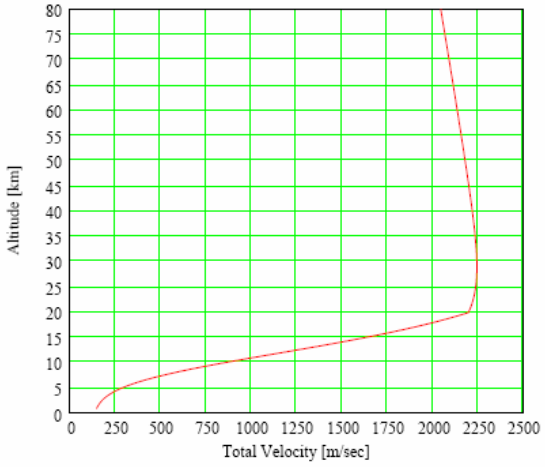

Fig. 8: Altitude vs. Velocity during Reentry and Separation of the P/L from Motor at 20 km

At an altitude of 4 km the recovery sequence starts with the deployment of a two-stage parachute system to provide a final velocity of approximately 15 m/s and safe landing.

3.3 VEHICLE DESIGN

Because of challenging problems concerning flight stability that occurred during the development of the SHEFEX vehicle the first design approach in Fig. 2 had to be changed. The asymmetric shape of the experiment induces a moment on the vehicle that will increase the angle of attack and lead to an instable flight.

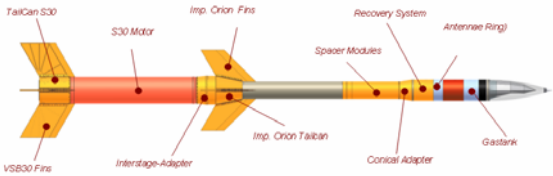

Fig. 9: New Design for SHEFEX rocket

All components that had to be changed to provide flight stability are marked yellow in Fig. 9 and are explained in the following sub-chapters.

3.3.1 2nd STAGE TAILCAN (FLARE & FINS)

The aerodynamic and stability studies on the SHEFEX reentry vehicle made a redesign of the Improved Orion standard tailcan necessary. After several aerodynamic studies of the DLR Institute of Aerodynamics and the Mobile Rocket Base the concept of a flare was chosen instead of using the standard boattail shape.

During these analyses the influence of fin size, flare length and angle, spacer modules and the hammerhead design on the flight stability and trim angle was evaluated. Also a comparison of results from VisualDATCOM, a semi-empirical software tool for rocket aerodynamics, and calculations with the DLR Euler- and Navier-Stokes Code at the Institute for Aerodynamics, DLR was conducted during this development process.

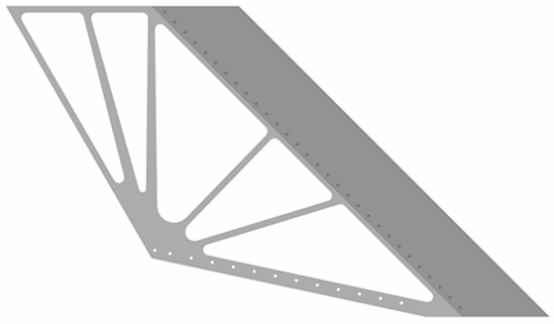

Fig. 10: New Fin Frame Design

The main problem for the flight stability is the difficulty to shift the centre of gravity closer to the tip of the vehicle. The heavy empty Improved Orion motor made it necessary to install also ballast mass in the front section of the vehicle, which has because of the total increasing mass a negative influence on the achieved apogee, respectively the velocity during reentry. The calculations showed that a trim angle around 3° is possible.

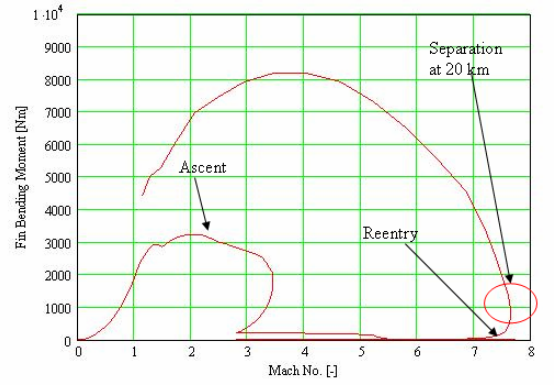

Fig. 11: Fin Bending Moment for Ascent and Reentry (AoA 5°)

Both, tailcan and fins had to be redesigned. For the fins a new approach concerning ribs and frame has been chosen that makes use of the evolution in manufacturing methods in the last decades. The stress that is induced in the fins by aerodynamic forces during ascent and especially during reentry is distributed in the frame more efficiently.

A similar fin design was successfully tested on the VSB-30 Rocket in October 2004.

For the layout of the fins, the bending moments that occur during the flight have to be regarded. In the ideal case the angle of attack in ascent is very low and during the reentry it is the trim angle. As worst case an angle of attack of 5° was assumed and the resulting bending moments were used for dimensioning the fin.

$$F_N = \frac{1}{2} \cdot \rho \cdot v^2 \cdot c_N \cdot A_{ref} = q \cdot c_N \cdot A_{ref} \qquad (1)$$

Aerodynamic forces, respectively bending moments were calculated analytically based on lift coefficients achieved from CFD calculations, see also eq. 1, but also with a semi-empirical software tool. In Fig. 11 the bending moments for 5° angle of attack is shown over the Mach number, respectively the flight. High bending moments would occur in the ascent for this angle of attack, which should not occur during a nominal flight. During reentry at point of separation the bending moment on one fin is around 1900 Nm. Higher moments would occur if the motor would be separated later in denser atmosphere.

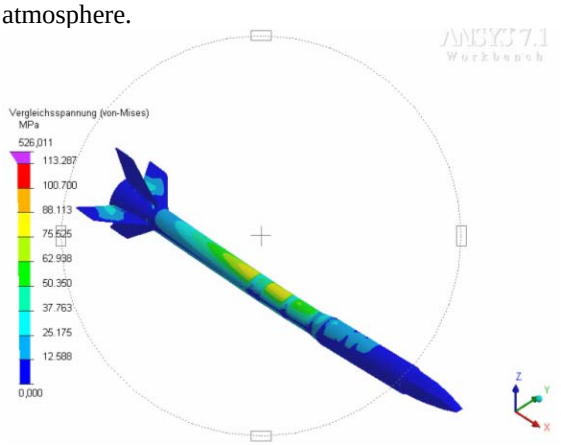

Fig. 12: Stress Analysis for the Reentry Vehicle (ANSYS DesignSpace™)

The basic structure of the tailcan consists of 4 rings that increase in diameter and shims that give stability against torsion. FEM analyses were conducted with ANSYS DesignSpace™ to show that the tailcan and vehicle can withstand the aerodynamic forces that occur during the hypersonic entry (see Fig. 12).

3.3.2 1st STAGE TAILCAN

Due to the new design of the 2nd stage tailcan with larger fins, a stability problem occurred for calculations on the ascent phase of the rocket. The standard S30 tailcan and fins had to be changed to a tailcan that was developed for the Brazilian VSB-30 and was tested successfully in October 2004. The larger fin set increases also the total mass of the vehicle.

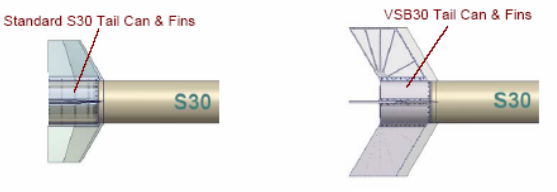

Fig. 13: Modification of 1st Tailcan Assembly

3.3.3 INTERSTAGE SEPARATION

As already mentioned in chapter 3.2.1 a passive separation system based on aerodynamic drag only is assumed to be insufficient. A passive spring-plunger system will guarantee save stage separation during coast phase. The arisen small gap between adapter and tailcan will increase the aerodynamic drag of the 1st stage and a smooth separation is ensured.

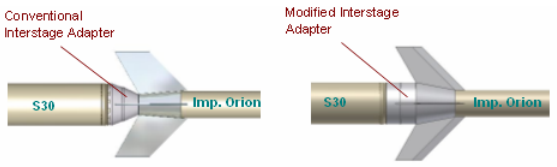

Fig. 14: Modification of Interstage Adapter

3.3.4 ATTITUDE CONTROL SYSTEM

The main sensor for the attitude control is a DMARS-R roll stabilised inertial platform. As low cost sounding rockets are usually spin stabilized at rates of up to 5 Hz during the boost phase, the use of gyro platforms on such vehicles is limited to those with a roll stabilised or de-spun outer gimbal which decouples the inertial sensors from the high roll rate. The DMARS is an inertial grade device which provides accurate attitude and position which is also an advantage for this mission as not only the reentry attitude is important but also the accelerations, rates and position which will provide the experimental data on the flight dynamics of the experiment form. The platform comprises in addition to the three gyros and three accelerometers, a computer which generates the navigation data and provides the attitude control signals for the cold gas system.

The main microcontroller in the ACS electronics performs data acquisition from the platform, the experiment electronics, GPS receiver, ignition and recovery system and pyrotechnic circuits computer and the general housekeeping within the ACS and assembles the various data packets in a PCM frame for telemetry. This computer also receives telecommands via dual redundant receivers for correction of manoeuvres or selective enabling of lateral and roll axes control. The experiment electronics also contains two microcontrollers which acquire and pre filter the data from 64 sensors in the experiment and housekeeping in the electronics and transfer these data packets to the telemetry controller. The control signals from the ACS activate the thrusters in a two level cold gas system with two thrusters each for the two lateral axes and four for the roll axis. The two levels provide high thrust for fast acquisition and low thrust for fine control. The gas system is mounted at the forward end of the vehicle for maximum lateral moment arm.

The baseline control strategy is a predefined manoeuvre according to the predicted nominal trajectory. In the event of the actual trajectory significantly differing from nominal, the predicted angle of attack will also be in error. Two solutions to this problem are incorporated in the system. A velocity vector calculation based on the navigation data of the DMARS platform could be used but as the problems of adequately qualifying such a routine in the flight computer are significant, the application of this solution can only be contemplated with in flight correlation with the radar trajectory data and activation by telecommand. An alternative is available in the calculation of flight vector from real-time radar data and transmission of the manoeuvre correction via telecommand.

The ACS electronics and service systems are supported by Electrical Ground Support Equipment (EGSE) which comprises external power and individual switching for the electronics, platform, stable oscillator for slant ranging, two telecommand receivers, two telemetry and one TV transmitters and a radar transponder. Three serial interfaces provide hardline communication via the umbilical with the platform, ACS electronics and GPS. In addition, a microcomputer controlled decommutator provides selection and distribution of data packets from the telemetry receiver or hardline to five personal computers for the display and archiving of:

- platform performance
- control system data
- main ACS housekeeping and recovery
- GPS and pyrotechnic circuits
- experiment data

3.3.5 S-BAND ANTENNA

To ensure data transmission also in the hypersonic reentry, a redesign of the existing blade antennae (S-Band, 2.25 GHz) became necessary. Former

flights with flat spin reentry showed that degradation of the antenna conductors and insulation occurred because of the high thermal stress. For a stable reentry the thermal strains on specific points of the vehicle will be even higher.

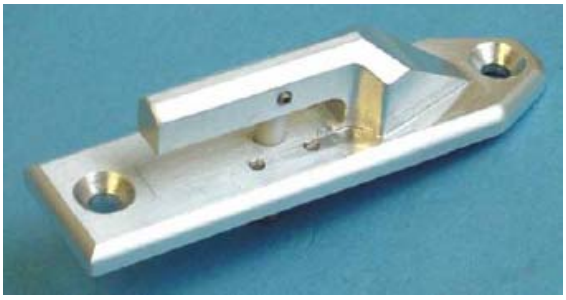

Fig. 15: Al-Prototype of Blade Antenna

The material for the usual blade antenna is a copper-beryllium-alloy (melting point 1030°C). The modified front body of the new antenna that is broadened and conically reduced at the end increases the expansion area. The Teflon-insulation of the conductor is changed to Ceramic to improve the thermal insulation.

The new blade antenna can also absorb more energy and the heat conduction to the payload modules is improved by a better attachment surface.

Tests were conducted at the L3K wind-tunnel at DLR, Köln-Porz and showed positive results concerning the temperature. A test antenna was also flown on the VSB-30 in October 2004.

3.3.6 RECOVERY SYSTEM

Because of the higher velocities that occur during the reentry for a stable flight of the SHEFEX vehicle, the time of the deployment of the first parachute was increased until the payload reached an altitude of 4 km instead of 6 km. The recovery system consists of a two-stage parachute system with a one stab chute and a tri-conical main parachute with an area of 24.6 m² and a floater with 220 l volume.

4. SUMMARY & OUTLOOK

With a successful flight of SHEFEX the DLR can prove that it is capable to gain real flight data of complex reentry experiments basing on low-cost sounding rocket flights. Due to the experience that is achieved during SHEFEX, the Mobile Rocket Base can also think about follow-up projects with a three-staged rocket to achieve even higher Mach numbers or test super combustion experiments.

5. REFERENCES

[1] Bryson, Arthur E., Jr.: *Control of Spacecraft and Aircraft*, Princeton University Press, 1994

[2] Gardner, A.D.; Hannemann, K.; Steelant, J.; Paull, A.: *Ground Testing of the HyShot Supersonic Combustion Flight Experiment in HEG and Comparison with Flight Data*, AIAA-2004-3345, 2004

[3] Jung, W.: *Baronesa Post-Flight Analysis*, DLR RB-MR, 2000

[4] Longo, J.M.A.; Püttmann, N.: *The DLR Sharp Edge Flight Experimen*t, Proceedings of the DGLR Jahrestagung, DGLR 2004-072, September 2004

[5] Montenbruck, O.; Markgraf, M.: *TEXUS-39 Orion GPS Tracking System Flight Report*, TEX39-DLR-RP-0001, DLR, 2001

[6] NASA AMES Space Projects Division: *http://cmex.arc.nasa.gov/SOAREX*, 2004

[7] Ratajczak, Thomas: *MATLAB®/Simulink®-Programmierung des dynamischen Verhaltens einer rotierenden Raketennutzlast / Entwurf und Simulation eines aktiven Kaltgas-Regelungssystems*, Universität der Bundeswehr, 2001

[8] Spaceflight Now: *www.spaceflightnow.com*, 2002

[9] University of Queensland: www.mech.uq.edu.au/hyper/hyshot, 2004

[10] Weihs, H.; Longo, J.; Gülhan, A.: *The Sharp Edge Flight Experiment*, DLR, 2003